Article

Identification and isolation of glucosytransferases (GT) expressed fungi using a two-photon ratiometric fluorescent probe activated by GT

Lei Feng, Ping Li, Jie Hou, Yonglei Cui, Xiangge Tian, Zhenlong Yu, Jing-Nan Cui, Chao Wang, Xiaokui Huo, Jing Ning, and Xiaochi Ma

Anal. Chem., **Just Accepted Manuscript** • DOI: 10.1021/acs.analchem.8b02857 • Publication Date (Web): 25 Oct 2018

Identification and isolation of glucosytransferases (GT) expressed fungi using a two-photon ratiometric fluorescent probe activated by GT

Lei Feng,[†,‡,§,#] Ping Li,[†,#] Jie Hou,[†,#] Yong-Lei Cui,[†] Xiang-Ge Tian,[†] Zhen-Long Yu,[†] Jing-Nan Cui,[§] Chao Wang,[†,§,*] Xiao-Kui Huo,[†] Jing Ning,[†] and Xiao-Chi Ma[†,*]

[†]College of Pharmacy, Academy of Integrative Medicine, Department of Microbiology, Dalian Medical University, Dalian 116044, P. R. China. Tel: +86-411-86110419; E-mail: wach_edu@sina.com (C. Wang); maxc1978@163.com (X.C. Ma)

[‡] Institute of Functional Materials and Molecular Imaging, College of Emergency and Trauma, Hainan Medical University, Haikou, 571199, China

[§] State Key Laboratory of Fine Chemicals, Dalian University of Technology, Dalian 116024, P. R. China

ABSTRACT: As well known, fungi as an important biocatalysis model of glucosylation, were widely applied for bioactive compounds glucosylation mediated by the intracellular glucosytransferases (GTs). However, there is no efficient method for the real-time detection of GTs and the rapid isolation of the target fungi strains with the high expression of GTs. In the present work, we firstly developed a two-photon ratiometric fluorescent probe N-(n-butyl)-4-hydroxy-1,8-naphthalimide (**NHN**) for detecting the glucosyltransferases activity and intracellular imaging of GTs. Under the UV light (365 nm), the transformed product of **NHN** mediated by intracellular glucosyltransferase displayed blue emission to guide the rapid isolation of fungal strains possessing over-expression of GTs from the complex soil samples. Finally, by using the fluorescent probe, two target fungi were isolated and identified to be *Rhizopus oryzae* and *Mucor circinelloides* by molecular analysis, and they exhibited a robust capability to regio- and stereospecific *O*-glycosylation. Our results fully demonstrated that **NHN** may be a promising tool for guiding real-time GTs activity in fungal strains, and even for developing natural fungal strains with GTs overexpression.

Glucosylation of molecules usually could enhance the water solubility and stability, facilitate the storage and accumulation in living cells, and even improve the chemical properties and bioactivities.[1-5] As now, chemical synthesis and bioconversion using glucosyltransferases (GTs, EC 2.4.1) both were the preparation approaches of bioactive glucosides.[6-11] GTs expressed in fungi, plant cells and even mammalian systems, could transfer an activated donor, uridine-diphosphate glucose (UDPG), onto target acceptor molecule.[12,13] Recently, glucosylation by GTs of prokaryotic systems, has become an interesting alternative in chemical synthesis of glucosides due to its high regio-, and stereo-selectivities and mild reaction conditions. Among many biocatalytic approaches, microbial transformation mediated by GTs has been well known to effectively obtain more active compounds and to achieve selective conversions.[14-17] However, some characterized fungi usually exhibited poor glucosylation capability. It is necessary to develop a novel approach to search for new fungi with high expressed GTs.

By virtues of real-time spatial high resolution and sensitive imaging with low autofluorescence, ratiometric fluorescence imaging technique presents the potent application for quantitative detection *in situ* and specific imaging of target enzymes, even ions.[18-26] 1,8-naphthalimide structures have been commonly employed in enzymatic sensing experiments, depended on the electron-donating capability of the substituent at C-4 of the naphthalic ring, which also displayed the

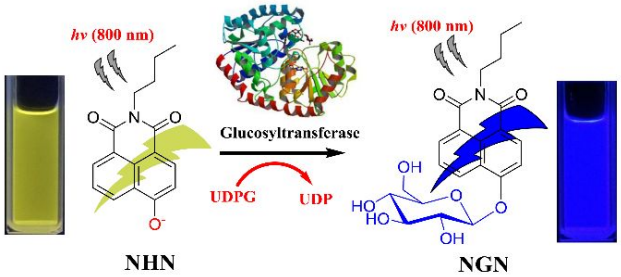

Scheme 1. Illustration of the **NHN** glucosylation mediated by GT.

photophysical property of two-photon absorptivity.[27-33] Therefore, according to these advantages of naphthalimide, we could readily realize the ratiometric detection of GTs *via* photophysical modulation through a glucose-induced change in C-4 substitution.

In the present work, a two-photon ratiometric fluorescent probe has been developed for real-time detection of GT on the basis of the formation of specific aglycone from N-(*n*-butyl)-4-hydroxy-1,8-naphthalimide (**NHN**), with the optical advantages including high photostablility, large Stoke shift and preferred fluorescence efficiency (Scheme 1). Furthermore, by using **NHN** for tracking fungal GTs, two potential wildtype fungi with the excellent capability of glucosylation were rapidly isolated from complex environmental samples, and then accurately identified by gene sequencing. Finally, their

glucosylation capabilities were further confirmed by various substrates and RT-PCR experiment.

EXPERIMENTAL SECTION

Materials and instruments. All the chemical reagents were purchased from Sigma Aldrich. Recombinant glucosyltransferase PlGT7 was gifted from Professor Jungui Dai of Institute of Materia Medica, Chinese Academy of Medical Sciences and Peking Union Medical College.[1] Recombinant Xylosyltransferase 1 (XYLT1), recombinant O-Mannosyltransferase 1 (POMT1) were purchased from Immune Clone Co., Ltd. Human uridine-disphosphate glucuronosyl-transferases (UGT1A1, UGT1A4, UGT2B4, UGT2B7); human N-acetyltransferase (NAT1, NAT2); human Sulfotransferases: (SULT2A1, SULT1B1); human Carboxylesterase (CES1b, CES1c, CES2) were purchased from Corning Incorporated Life Sciences. Human catechol-*O*-methyltransferase (DOMT) were gifted from Ling Yang professor of Lab of Pharmaceutical Resource Discovery, Dalian Institute of Chemical Physics, Graduate School of the Chinese Academy of Sciences. Leucine arylamidase from porcine kidney (LAP) was purchased from sigma-aldrich.

NMR spectra were measured using Bruker-600, 500 with tetramethylsilane (TMS) as the internal standard (Bruker, USA). HR-MS data were obtained on an Agilent 1290 infinity 6540 UHD accurate mass Q-TOF MS (Agilent, USA). Constant temperature incubator shaker (ZHWY-2012C) was the production of by Shanghai Zhicheng Analytical Instrument Co. Ltd (P. R. China). Fluorescence microscopic imaging was conducted with Olympus FV 1000 MPE/FV-1000 FLIM Confocal Microscope (Olympus, Japan). The bioassay solutions in 96-well plates were also analyzed using a BioTek Synergy H1 microplate reader (BioTek, USA). The dissociation constant (KD) between the fluorescent probe **NHN** and the enzyme GT was determined to on the basis of Microscale thermophoresis (MST) using the NanoTemper monolith NT.115 instrument (Nano Temper, Germany).

Synthesis of probe NHN. The fluorescent probe **NHN** was synthesized following the reported procedure as the synthetic route displayed in Scheme 2.[27,31,34]

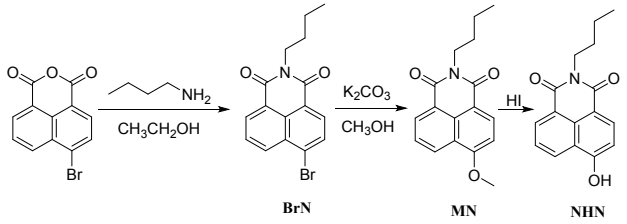

Scheme 2. The synthetic route of **NHN**.

*Synthesis of compound **BrN***. 4-bromo-1,8-naphthalic anhydride (1 g, 3.62 mmol) and *n*-butylamine (0.291 g, 3.98 mmol) were dissolved in ethanol (30 mL). The reaction mixture was stirred and refluxed for 8 h. After cooling to room temperature, the mixture was poured into ice water; the precipitate was washed with water and ethanol, and dried to yield 1.09 g of a yellowish-color solid (yield 90.9%)(Figure S1-S3).

*Synthesis of compound **MN***. A mixture of compound **BrN** (0.8 g, 2.42 mmol) and K_2CO_3 (2.54 g, 18.4 mmol) in 30 mL CH_3OH was refluxed for 6 h. After cooling to room temperature, the precipitate was filtered, washed with water and dried to yield compound **MN** as a yellow-color solid (0.585 g, yield: 85.5%) (Figure S4-S6).

*Synthesis of compound **NHN***. A mixture of compound **MN** (0.3 g, 1.06 mmol) and 10 mL concentrated HI (55−58%) was refluxed for 14 h. After cooling the mixture was poured into water; the precipitate was isolated, washed with water, and dried to yield 0.239 g of the yellow needles solid (yield 83.8%). (Figure S7-S9).

Preparation of 4-O-*β*-D-glucopyranosyl-N-butyl-1,8-naphthalimide (NGN) by the glucoylation of NHN. The isolated filamentous fungi *R. oryzae* was pre-incubated in potato medium to get enough fungi cells for the glucosylation experiment. After filtration, the fungi cells were suspended in the glucosylation medium. The glucosylation medium was sodium phosphate buffer: 13.62 g NaH_2PO_4, 2.36 g NaOH, and 20 g D-glucose in 1000 mL water. 1.5 g *R. oryzae* AS 3.2380 fungus cells were pre-incubated in the glucosylation medium (200 mL), 30 ºC, 130 rpm for 12 h. Then, **NHN** substrates (30 mg) dissolved in acetone were injected into the medium with the continued incubation for 24 h. When the fungus cells were filtered, the incubation culture was subjected to a MCI column, which was eluted by 30% ethanol aqueous, 50% ethanol aqueous, and 95% ethanol, successively. The **NGN** could be obtained in the 50% ethanol aqueous elution with the purity > 95%, the structure of which was determined on the basis of widely spectroscopic data (Figure S10-S14).

Determination of the quantum yield (QY). The fluorescence quantum yields for compounds with Absolute PL Quantum Yield Spectrometer (HAMAMATSU C11347). The PL Quantum Yield (Φ) is expressed as the ratio of the number of photons emitted from molecules (PN_{em}) to that absorbed by molecules (PN_{abs}).

$$\Phi = PN_{em}/PN_{abs} \quad \ldots\ldots (1)$$

Glucosyltransferase activity analysis. The present fluorescence assay was performed with the presence of **NHN** using the purified glucosyltransferase PlGT7.[5] The glucosyltransferase (30 μg/mL) was dissolved in 200 μL phosphate buffer (pH 7) together with **NHN** (10 μM) and uridine-diphosphate glucose (UDPG, 300 μM), which was incubated at 37 ºC for 30 min. **NHN** (10 μM) was obtained when the **NHN** stock solution (1 mM, DMSO) was added into the phosphate buffer with the DMSO volume < 1%, which could improve the solubility of **NHN** and keep the activity of GT. Then, 100 μL acetonitrile was added to stop the enzymatic reaction. The reaction solutions were measured the fluorescence spectra using BioTek Synergy H1 microplate reader (λ_{ex} 398/λ_{em} 446 nm and λ_{ex} 398/λ_{em} 556 nm).

Fluorescence responses of **NHN** (10 μM) to the concentration of GT were performed upon addition of increasing concentration of GT (0 − 90 μg/mL) in phosphate buffer for 30 min. Meantime, fluorescence responses of **NHN** (10 μM) to the incubation time were studied upon the addition of GT (30 μg/mL) in phosphate buffer for incubation time 0 – 80 min with acetonitrile (33%, *v/v*) to terminate the enzymatic reaction (λ_{ex} 398/λ_{em} 446 nm, λ_{ex} 398/λ_{em} 556 nm, gain value = 80%, 37 °C). The relationship was analyzed on the basis of the fluorescence intensities ratio (I_{446}/I_{556}).

The enzymatic selectivity experiments towards different enzymes (30 μg/mL) were preformed according to their enzymatic reaction conditions,[35-38] including recombinant Xylosyltransferase 1 (XYLT1), recombinant O-

Mannosyltransferase 1 (POMT1), Uridine-disphosphate glucuronosyl-transferases: UGT1A1, UGT1A4, UGT2B4, UGT2B7; N-acetyltransferase: NAT1, NAT2; Sulfotransferases: SULT2A1, SULT1B1; Catechol-*O*-methyltransferase: DOMT, Carboxylesterase: CES1b, CES1c, CES2; and leucine arylamidase: LAP. The fluorescence intensities ratio (I_{446}/I_{556}) was studied on the basis of the fluorescence emission (λ_{ex} 398/λ_{em} 446 nm, λ_{ex} 398/λ_{em} 556 nm). The influence of metal ions on the fluorescence emission of **NHN** and **NGN** and the activity of GT were measured with the presence of K^+, Mg^{2+}, Fe^{3+}, Fe^{2+}, Ba^{2+}, Ca^{2+}, Mn^{2+}, Sn^{4+}, Zn^{2+}, Ni^{2+}, Cu^{2+}, SO_4^{2-}, NO_3^-, CO^{2-} (each 2 mM).

In order to estimate the kinetic parameters of **NHN** for GT, the reaction kinetics were performed. Briefly, **NHN** (0−60 μM) was incubated with GT for 30 min which ensured less than 20% of substrate was metabolized, and the formation rates of **NGN** were in relation to incubation time and protein concentration in the linear range. The GT stock solution was prepared to be 10 mM in DMSO, which was added into the GT enzymatic reaction system with DMSO < 1%. The apparent K_m and V_{max} values were calculated from nonlinear regression analysis of experimental data according to the Michaelis-Menten equation.

The V_{max} represents the maximum rate and K_m is the substrate concentration at the half-maximal rate. Kinetic constants were obtained using Origin 7.5 (origin Lap Corp. Northampton. MA.USA) and produced as the mean ± SD of the parameter estimate.

Isolation of fungi with the guidance of NHN. The soil sample obtained from the farmland (Dalian, China) was used as the source for the fungi purification. The soil sample (10 g) was extracted by sterile water (50 mL). After the centrifugation of the solid residue, the clear supernatant water was well-distributed on the PDA medium (Potato Dextrose Agar medium) containing penicillin and streptomycin (50 mg/L), which was used to inhibit the propagation of prokaryotes. The culture dishes were stored at 30 ºC for 48 h. When the fungal colonies were observed on the PDA medium in the culture dish, **NHN** solutions (50 μM, phosphate buffer) were added upon the fungal colonies for co-incubation. After the incubation of 1 hour, the mix fungal colonies were excited under UV light at 365 nm, which displayed the blue or yellow fluorescent colonies. On the basis of the fluorescence spectrum of **NGN** (λ_{em} 446 nm), the fungal colonies displayed blue fluorescence emission were determined to be the target fungi with the expression of GT. Then, under the aseptic condition, single colonies with blue fluorescence emission were picked up and subjected on the PDA medium for the culture at 30 ºC for 48 h. When the fungal colonies were observed, **NHN** was applied to identify the target fungi again. And, the target fungi were picked up repeat until the purify fungi were obtained. Finally, two fungal colonies displayed significant blue fluorescence emission under the UV light irritation (365 nm) were obtained as F-1 and F-2 fungi.

Molecular analysis of two isolated fungi. The filamentous fungi (F-1, F-2) were grown at PDA medium and was assayed using 18S rRNA and ITS sequencing (Figure S15, Table S1). All sequences of the ITS and 18S rRNA of each isolate were aligned using software ApE. The molecular analysis of the ITS1-5.8S-ITS2 and 18S rRNA regions of fungal strains F-1, F-2 were performed by searching databases using BLAST (http://www.ncbi.nlm. nih.gov/BLAST/). Evolutionary analyses of two isolated fungi strains on the basis of 18S rRNA and ITS sequencing were conducted in MEGA7.

Confocal microscopic imaging of fungi strains. Two isolated fungi *R. oryzae* (F-1) and *M. circinelloides* (F-2) were incubated in YPG medium at 30 ºC for 12 h. Fluorescent probe **NHN** (50 μM) was added and incubated for 8 h. The hyphostromas were filtered and washed by sterile water and re-suspended in 0.1 M PBS, pH 7 and spotted on poly-L-lysine pre-treated glass slides and immobilized with coverslips. Fungal imaging tests were conducted with Olympus Confocal Microscope with the excitation wavelength at 800 nm and emission wavelength at 460 − 500 nm, and 520 − 560 nm, respectively.

Glucosylation of different substrates by *R. oryzae*. Nine natural compounds kaempferol (**1**), apigenin (**2**), 4-methyldaphnetin (**3**), emodin (**4**), triptophenolide (**5**) and environmental pollutants estrogens ethinylestradiol (**6**), 17*α*-estradiol (**7**), 17*β*-estradiol (**8**), and estrone (**9**) were used as the substrates to be glucosylated by the isolated filamentous fungi *R. oryzae*, following the procedure of **NHN** glucosylation as abovementioned. Each substrate (2 mg) was transformed by *R. oryzae* in 100 ml incubation culture. After the filtration of fungal hyphostroma, the cultures containing substrates and corresponding glucosides were analyzed using HPLC-DAD and HR-MS. The HPLC conditions were as followed: CH_3OH-H_2O (10:90 – 100:0, 0 – 50 min), follow rate 1 mL/min, detected at 210 nm. Comparison of the peak area between the substrates and glucosides was used to calculate the conversion rates.

Reverse transcription-polymerase chain reaction (RT-PCR) experiment of GTs in *R. oryzae*. Total RNA was extracted using TRIzol reagent according to the kit protocol (TaKaRa Bio, Dalian, China). cDNA was reverse-transcribed using the PrimeScript RT Reagent Kit (TaKaRa Bio, Dalian, China) according to the manufacturer's instructions. PCR analysis was performed on aliquots of the cDNA preparations to detect gene expression. Primer pairs were as shown in Table S2. The polymerization reaction was performed in an Aglient SureCycler 8800 under the following conditions: an initial denaturation of 3 min at 98 °C; 35 cycles of 30 s at 95 °C, 30 s at 60 °C and 30 s at 72 °C; after the 35 cycles, an extra extension step of 15 min at 72°C was added, followed by cooling at 16 °C at the end of this program. Amplification products were analyzed on 1.5% agarose gel electrophoresis, stained with ethidium bromide, and photographed under ultraviolet light.

RESULTS AND DISCUSSION

Fluorescent characteristic of NHN towards GT. According to the substrate preference of glycosyltransferase, the 4-OH of naphthalimide could be as the vital reaction site of GT. **NHN**, with the two-photon ratiometric fluorescent characteristics, was used as the best preferred substrate of GT, for real-time monitoring and visualizing the GTs of fungi. The phenolic hydroxyl group at C-4 position of **NHN** was a good electron donor, which could accept the glucosyl group from UDPG in the presence of GT (Scheme 1). The glucosylated product **NGN** was also detected in the enzymatic solutions using HPLC-DAD (Figure S16), and its chemical structures was confirmed on the basis of 1D-, 2D-NMR and HRMS, respectively. Because the 4-OH triggered a strong intramolecular charge transfer (ICT) effect upon photon excitation in its structure,[39] the glucosylation of 4-OH induced

the significant changes of both absorption and emission of the 4-O-*β*-D-glucopyranosyl-N-butyl-1,8-naphthalimide (**NGN**). Compared with the moderate emission of **NHN** (λ_{em} 556 nm, Φ = 0.183), **NGN** as a water-soluble product, displayed a stronger fluorescence emission at λ_{em} 446 nm (Φ = 0.788) (Figure S17). It was reported that 4-O-*β*-D-galactopyranosyl-N-butyl-1,8-naphthalimide has been developed for the detection of *β*-galactosidase (**NI-βGal**), with the N-(*n*-butyl)-4-hydroxy-1,8-naphthalimide as the sensing product.[29] Although our product (**NGN**) had same planar structure with **NI-βGal**[31], the configuration of 4α-OH of glucopyranosyl moiety in **NGN** is different with that of **NI-βGal**. **NGN** and **NI-βGal** possessing the similar chemical structure displayed the similar fluorescent properties at λ_{ex} 350/λ_{em} 446, and λ_{ex} 365/λ_{em} 440 nm, respectively, which also confirmed the glucosylation of **NHN** by GT.

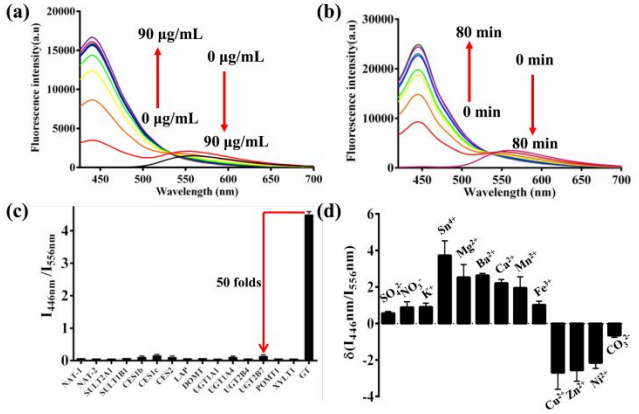

Figure 1. (a) Fluorescence spectra changes of **NHN** (10 μM) upon addition of increasing concentration of GT (0 − 90 μg/mL). (b) Fluorescence spectra changes of **NHN** (10 μM) upon addition of GT (30 μg/mL) in phosphate buffer for incubation time 0 – 80 min. (c) Fluorescence intensities ratio (I_{446}/I_{556}) of **NHN** (10 μM) upon addition of different enzymes (30 μg/mL). (d) The influence of various ions (2 mM) on the enzymatic glucosylation of **NHN**. (λ_{ex} 398/λ_{em} 446 nm, λ_{ex} 398/λ_{em} 556 nm, gain value = 80%, Enzymatic reaction was performed in KH_2PO_4-K_2HPO_4 buffer (pH 7) and terminated with acetonitrile (33% *v/v*), UDPG 0.3 mM, 37 °C; **NHN** were resolved in DMSO as stock solution, which was added into the GT KH_2PO_4-K_2HPO_4 buffer solution with DMSO volume < 1%).

Fluorescence behavior of NHN towards GT under different conditions. The fluorescence behavior of **NHN** mediated by GT at the different concentrations (0 − 90 μg/mL) was investigated. Figure 1a showed that the emission at 446 nm corresponding to **NGN** increased while the original emission at 556 nm of **NHN** decreased following with the increase of GT concentrations. And a good liner relationship was observed between the fluorescence intensities ratio (I_{446}/I_{556}) and concentrations of GT (Figure S18). Additionally, the established calculation curve displayed an excellent accuracy for the GT activity assay using the known GT concentration (Table S3). Absorption spectra of **NHN** upon additions of different amounts of GT (0 − 90 μg/mL) in phosphate buffer for 30 min were also recorded, which displayed the change of **NGN** and **NHN** similarly to Figure 1a (Figure S19).

NHN was designed as the fluorescent probe for selectively sensing GTs. Thus, the enzymatic selectivity and stability characteristics of **NHN** were investigated between GT and other conjugases (Xylosyltransferase 1 (XYLT1), O-Mannosyltransferase 1 (POMT1), Uridine-disphosphate glucuronosyl-transferases: UGT1A1, UGT1A4, UGT2B4, UGT2B7; N-acetyltransferase: NAT1, NAT2; Sulfotransferases: SULT2A1, SULT1B1; Catechol-*O*-methyltransferase: DOMT) and hydrolases (Carboxylesterase: CES1b, CES1c, CES2; Leucine arylamidase: LAP). Especially, XYLT1, POMT1 and UGTs were the similar glycosyltransferases, in comparison with GT. As shown in Figure 1c, the fluorescence intensity ratio I_{446}/I_{556} of GT enzymatic system was approximately 50-fold than those of other enzymes, which displayed a high selectivity of **NHN** towards GT as well as the stability of **NHN** in the presence of hydrolase. Furthermore, hydrolysis of **NGN** mediated by various glycoside hydrolases (0.1 U), has been investigated, which indicated the well stability of NGN in the presence of glycoside hydrolases, such as *β*-glucosidases, *α*-glucosidase, and *β*-glucuronidase (Figure S20). The enzymatic kinetics of **NHN** glucosylation mediated by GT gave a Michaelis-Menten enzymatic reaction with the V_{max} 0.06145 ± 0.002814 μmol/min/mg and K_m 6.748 ± 1.082 μM (Figure S21), which displayed a better affinity than those known substrates.[5] Additionally, using the Microscale thermophoresis binding assay as a technique, the KD for **NHN** binding to GT was calculated to be 76 μM (Figure S22).

The influence of ions on the fluorescence responses of NHN. As shown in Figure S23, no influence of ions including metal and acid ions on fluorescence responses of **NHN** and **NGN**, was observed. However, when these ions were added into the incubation system, they displayed potential influence on the glucosylation of **NHN** mediated by GT (Figure 1d). Under relatively high concentration of ions (2 mM), some of common ions such as Sn^{4+} and Mg^{2+} could remarkably improve the GT activity. However, Cu^{2+}, Zn^{2+}, Ni^{2+}, and CO_3^{2-} inhibited the glucosylation of **NHN** significantly. Moreover, the influence of ions towards GT activity was similar to the previous reports, which meant that **NHN** for sensing GT was very reliable.[5,40]

The rapid isolation of GT expressed fungi with the guidance of NHN. Recently, more and more fungi were applied as the catalytic systems to prepare various glycoside derivatives from medicinal compounds.[41,42] And many GTs has been obtained and characterized from natural fungi. However, the tedious screening experiment of target fungi strains from complex sample would be challenged for researchers. Therefore, the efficient detection of GTs in fungi is very important to find the novel typical fungi with over-expressed GTs. On the basis of data above mentioned, **NHN** was further applied for the real-time detection of GTs in fungi, which could effectively guide the rapid isolation of fungi with high glucosylation capability from the complex soil samples.

The soil sample from the farmland of Dalian Medical University was used for further purification of target fungi. The soil sample was extracted by sterile water and then well-distributed on PDA medium (Potato Dextrose Agar medium) containing penicillin and streptomycin (50 mg/L). When the fungal colonies were observed on PDA medium (Figure 2), the KH_2PO_4-K_2HPO_4 (pH 7) solution of **NHN** (50 μM, 1% DMSO), were added into the culture dish. Then, the mix fungal colonies were excited under UV light 365 nm, which gave the blue or yellow fluorescence colonies after the incubation of 1 h (Figure 2). On the basis of fluorescence

spectra of **NGN** (λ_{em} 446 nm), single colony isolation technique was performed to select the blue fluorescence colonies. Finally, two fungal colonies were obtained with significant blue fluorescence emission under UV light irritation (365 nm) (Figure 2f, 2i), which were deduced to be GTs engineering fungi strains (F-1, F-2). On the other hand, the negative fungi strains were also isolated, which displayed no blue emission in the presence of **NHN** under the UV light (Figure S24). Furthermore, the molecular analysis of the ITS1-5.8S-ITS2 and 18S rRNA regions of fungal strain (F-1) showed high similarity (95%, 96%) to the species *Rhizopus oryzae* by searching databases using BLAST (http://www.ncbi.nlm.nih. gov/BLAST/). Similarly, fungal strain (F-2) also displayed high similarity to the species *Mucor circinelloides*. As shown in Figure S25-S28, the phylogenetic clades formed on the basis of ITS1-5.8S-ITS2 and 18S rRNA genes using MEGA7 were applied to identify *R. oryzae* and *M. circinelloides*, respectively.

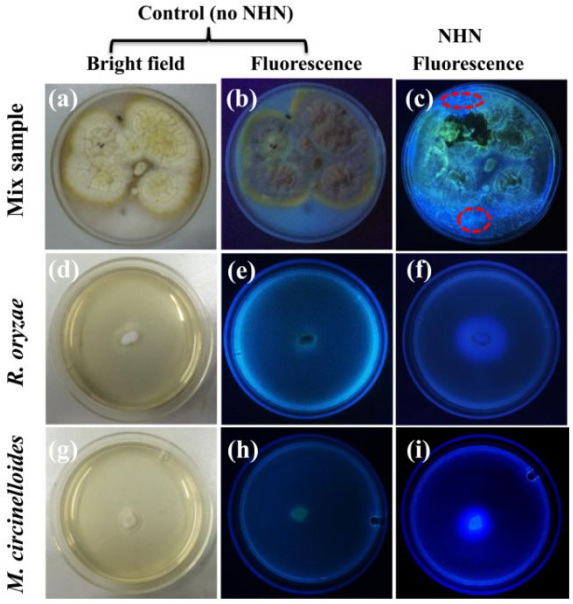

Figure 2. Fluorescent colony imaging of fungi in the presence of NHN (50 μM) under UV light at 365 nm. Mix sample (soil sample, a-c), R. oryzae (fungus F-1, d-f), and M. circinelloides (fungus F-2, g-i).

The fluorescent imaging of fungi with NHN. We further evaluated the potential application for two-photon ratiometric fluorescence imaging intracellular GT in *R. oryzae* and *M. circinelloides*. After the incubation of two fungal strains for 12h at 30 °C, **NHN** (50 μM) solution containing 1% DMSO was added for the continuous incubation of 8h, respectively. After the cleanout of culture media, the hyphostromas of *R. oryzae* and *M. circinelloides* were subjected to a confocal microscopy for fluorescence imaging excited by two-photon (λ_{ex} 800 nm), respectively. As shown in Figure 3, the images of two fungi displayed significant fluorescent emission excited by two-photon (λ_{ex} 800 nm). Additionally, one-photon confocal microscopy images of two fungi also displayed the fluorescent emissions of **NHN** and **NGN** (Figure S31). Compared with the one-photon images, two-photon images showed stronger fluorescent emission, which indicated the absolute advantage of two-photon in the imaging of intracellular GTs.

The glucosylation of **NHN** by *R. oryzae* was also confirmed by HPLC-DAD without other metabolites (Figure S32). As a ratiometric fluorescent probe, **NHN** was applied to quantitatively determine the glucosylation capability of two isolated fungi. Furthermore, as a fluorescent probe to sense endogenous GT in fungus, **NHN** displayed no cytotoxicity against fungal cells (*R. oryzae*) under different concentrations (0, 10, 50, 100 μM) and co-incubation time (4 h, 8h, 12h, and 24h) (Figure S33). Compared with the fluorescence emission of *R. oryzae*, *M. circinelloides* displayed weaker fluorescence response to **NGN**. Generally, the ratio value (Figure 3d, I_{450}/I_{550}) of *R. oryzae* was twofold of *M. circinelloides* (Figure 3h, I_{450}/I_{550}), which indicate the expression difference of GTs in two fungal strains. In the same way, the one-photon radiometric images (Figure S31d, S31h) also indicated the more expressed GT of *R. oryzae* than that of *M. circinelloides*.

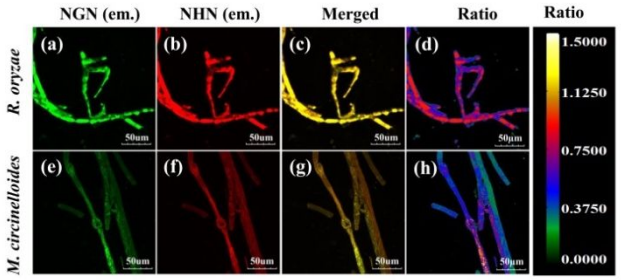

Figure 3. Two-photon confocal microscopy images of *R. oryzae* and *M. circinelloides* (λ_{ex} 800 nm; a, e: λ_{em} 460 − 500 nm; b, f: λ_{em} 520 − 560 nm; c, g: merge; d, h: ratio) incubated with NHN (50 μM, 1% DMSO) for 8 h at 30 °C. Scale bar 50 μm. Control group without NHN (Figure S29, S30).

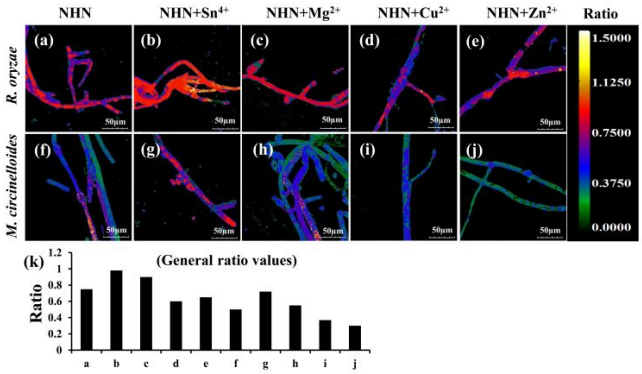

Figure 4. Two-photon ratiometric confocal microscopy images of *R. oryzae* and *M. circinelloides* in the presence of different metal ions (a, f: GT control; b, g: Sn^{4+}; c, h: Mg^{2+}; d, i: Cu^{2+}; e, j: Zn2+) and the corresponding general ratio values (k). The ratiometric images displayed the ratios of emission intensities collected at λ_{em} 460 − 500 nm and λ_{em} 520 − 560 nm with the λex 800 nm. Scale bar 50 μm.

The present investigation indicated that the glucosylation of **NHN** by GT was influenced significantly by several metal ions (Figure 1d), which was similar to the reported results.[5,38] Therefore, the influences of metal ions on the intracellular GT's activity in *R. oryzae* and *M. circinelloides* was studied using **NHN** as the substrate. According to the previous results (Figure 1d), Sn^{4+} and Mg^{2+} were applied as the activators for the GT activity. On the other hand, Cu^{2+} and Zn^{2+} were added into the culture of two isolated fungi as the inhibitor for the GT activity. When the two-photon confocal microscopy

images were obtained, the ratio images indicated that metal ions displayed similar influences on the glucosylation of **NHN** mediated by *R. oryzae* and *M. circinelloides* (Figure 4). The Sn^{4+} could increase the emission intensity corresponding to the significant production of **NGN**, according to the general ratio values 0.98 (*R. oryzae*) and 0.72 (*M. circinelloides*).

Meantime, the Mg^{2+} could enhance the glucosylation capability of two fungi moderately. On the other hand, Cu^{2+} and Zn^{2+} could decrease the ratio values moderately, which meant the less production of **NGN**. All of the fluorescence images suggested the activation of GT by Sn^{4+} and Mg^{2+} and the inhibitory effect Cu^{2+} and Zn^{2+} on GT, which would be helpful for the micro transformed glucosylation. Additionally, the significant influence of metal ions on the glucosylation capability of fungi, were consisted with that of *in vitro* experiment (Figure 1d). Therefore, these evidences indicated that the two-photon ratiometric fluorescent probe **NHN** to detect intracellular GTs was reliable and effective.

The confirmation of glucosylation capability of fungi by RT-PCR and various substrates. The glucosylation capability of *R. oryzae* was confirmed using some medicinal compounds as GT substrates including kaempferol (**1**), apigenin (**2**), 4-methyldaphnetin (**3**), emodin (**4**), triptophenolide (**5**) and environmental pollutants estrogens ethinylestradiol (**6**), 17*α*-estradiol (**7**), 17*β*-estradiol (**8**), and estrone (**9**). After the incubation of *R. oryzae* with these substrates for 48h, the corresponding glucoside derivatives were detected by HPLC and MS (Figure S34-S51), and their conversion rates were determined as shown in Figure 5a, 5b. Most of the substrates could be transformed to their corresponding glucosides with high conversion rates of 70%−95%. However, the multiple phenolic compounds such as compounds (**2**−**4**) were converted to glucosides with the approximate rates of 30%, which may be deduced by the affinity distinction between substrates and GT protein.

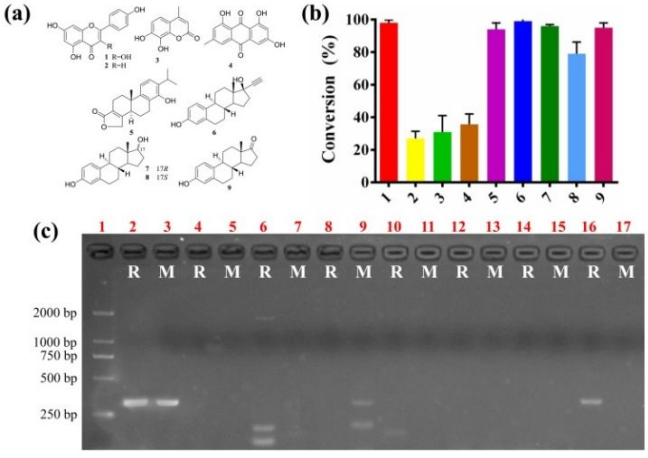

Figure 5. (a) The chemical structures of various substrates; (b) the yields of Glucosylation by *R. oryzae*. (c) RT-PCR of different glycosyltransferases in *R. oryzae* (R) and *M. circinelloides* (M). Protein marker (1), 18S (2, 3), UGT58A1 (4, 5), UGT59A1 (6, 7), Asm25 (8, 9), ElmGT (10, 11), UrdGT1a (12, 13), UrdGT1b (14, 15), and UrdGT1c (16, 17).

In order to confirm the expression of GTs in *R. oryzae* and *M. circinelloides*, RT-PCR experiment has been performed for several GTs proteins, including UGT59A1, ElmGT, UrdGT1c and ElmGT, all of which were obtained from microorganisms. As shown in Figure 5c, RT-PCR experiment indicated that proteins similar to UGT59A1, ElmGT, and UrdGT1c were expressed in *R. oryzae*. Asm25 alike protein was expressed in *M. circinelloides*. Especially, the UGT59A1 expressed in *R. oryzae* was a GT enzyme isolated from fungus *Rhizopus japonicas*, previously.[41] So, it was reasonable that *Rhizopus oryzae* and *Rhizopus japonicas* as the fungal strains of *Rhizopus* genus expressed the same GT UGT59A1.

Thus, both glucosylation of various compounds and RT-PCR analysis fully confirmed that *R. oryzae* and *M. circinelloides* possessed abundant GTs and excellent glucosylation capability, which strongly proved our fluorescent probe to be useful in rapidly discovering target fungi with over-expressed GTs from complex samples.

CONCLUSIONS

In summary, a two-photon ratiometric fluorescent method was developed for detecting GTs activity in fungal samples by using our designed probe. And this probe can serve as a convenient one-step straight forward assay for GTs detection, as well as provide a powerful approach for real-time tracking GTs-rich fungal strains. Finally, using our strategy, two targeted filamentous fungi were efficiently obtained, which were identified as *R. oryzae* and *M. circinelloides* by molecular analyses. These fungi as the novel transformation models, exhibited the robust capability to regio- and stereospecific *O*-glycosylation. Our strategy herein could offer the new quantitative approach for rapid isolation and imaging the fungi with high level of GTs from the complex samples.

ASSOCIATED CONTENT

Supporting Information

The supplementary figures, and spectroscopic spectra of compounds. This material is available free of charge via the Internet at http://pubs.acs.org.

AUTHOR INFORMATION

Corresponding Author

*Chao Wang
Fax: + 86 411 86110419;
E-mail address: wach_edu@sina.com;
*Xiaochi Ma
Fax: + 86 411 86110419;
E-mail address: maxc1978@163.com

Author Contributions

# L. Feng, P. Ling, and J. Hou contributed equally to this work.

Notes

The authors declare no competing financial interest.

ACKNOWLEDGMENT

We are grateful for the financial support from the National Natural Science Foundation of China (No. 81872970, 81622047, 81503201), Distinguished professor of Liaoning Province and the State Key Laboratory of Fine Chemicals (KF1603, KF1705) for financial support.

REFERENCES

(1) Zhou, M. Q.; Thorson, J. S. Asymmetric enzymatic glycosylation of mitoxantrone. *Org. Lett.* **2011**, *13*, 2786–2788.
(2) Zhou, M. Q.; Hou, Y. P.; Hamza, A.; Zhan, C. G.; Bugni, T. S.; Thorson, J. S. Probing the region-specificity of enzyme-catalyzed steroid glycosylation. *Org. Lett.* **2012**, *14*, 5424–5427.

(3) Xie, K. B.; Chen, R. D.; Li, J. H.; Wang, R. S.; Chen, D. W.; Dou, X. X.; Dai, J. D. Exploring the catalytic promiscuity of a new glycosyltransferase from *Carthamus tinctorius*. *Org. Lett.* **2014**, *16*, 4874–4877.

(4) Gutmann, A.; Krump, C.; Bungaruang, L.; Nidetzky, B. A two-step O- to C-glycosidic bond rearrangement using complementary glycosyltransferase activities. *Chem. Commun.* **2014**, *50*, 5465–5468.

(5) Sun, L. L.; Chen, D. W.; Chen, R. D.; Xie, K. B.; Liu, J. M.; Yang L.; Dai, J. G. Exploring the aglycon promiscuity of a new glycosyltransferase from *Pueraria lobata*. *Tetrahedron Lett*. **2016**, *57*, 1518–1521.

(6) Mikula, H.; Skrinjar, P.; Sohr, B.; Ellmer, D.; Hametner, C.; Frohlich, J. Total synthesis of masked Alternaria mycotoxinsdsulfates and glucosides of alternariol (AOH) and alternariol-9-methyl ether (AME). *Tetrahedron* **2013**, *69*, 10322–10330.

(7) Kajjout, M.; Zemmouri, R.; Eddarir, S.; Rolando, C. An efficient access to (*Z*)-*β*-fluoroallyl alcohols based on the two carbon homologation of aromatic aldehydes by HornereWadsworthEmmons reaction with 2-(diethoxyphosphinyl)-2-fluoro-ethanethioic acid, S-ethyl ester followed by reduction with sodium borohydride. *Tetrahedron* **2012**, *68*, 3225–3230.

(8) Sun, Y.; Zhang, J.; Li, C.; Guan, H.; Yu, G. Synthesis of glycoglycerolipid of 1,2-dipalmitoyl-3-(*N*-palmitoyl-6'-amino-6'-deoxy-*α*-D-glucosyl)-*sn*-glycerol and its analogues, inhibitors of human Myt1-kinase. *Carbohyd. Res.* **2012**, *355*, 6–12.

(9) Shimoda, K.; Kubota, N.; Hamada, M.; Sugamoto, M.; Ishihara, K.; Hamada, H. Glucosylation of taxifolin with cultured plant cells. *Nat. Prod. Commun.* **2013**, *8*, 903–904.

(10) Miranda-Molina, A.; Marquina-Bahena, S.; López-Munguía, A.; Álvarez, L.; Castillo, E. Regioselective glucosylation of inositols catalyzed by *Thermoanaerobacter* sp. CGTase. *Carbohyd. Res.* **2012**, *360*, 93–101.

(11) Li, N.; Miao, J.; Li, J.; Zhao, Y. R.; Li, H. M.; Dai, Y. Q.; Huo, Q.; Wu, C. Z.; Ma, T. Enzymatic synthesis of novel corylifol A glucosides *via* a UDP glycosyltransferase. *Carbohyd. Res.* **2017**, *446–447*, 61–67.

(12) Kim, J. H.; Kim, B. G.; Park, Y.; Ko, J. H.; Lim, C. E.; Lim, J.; Lim, Y.; Ahn, J. H. Characterization of flavonoid 7-O-glucosyltransferase from Arabidopsis thaliana. *Biosci. Biotechnol. Biochem*. **2006**, *70*, 1471–1477.

(13) Thibodeaux, C. J.; Melancon III, C. E.; Liu, H. W. Natural-Product sugar biosynthesis and enzymatic glycodiversification. *Angew. Chem. Int. Ed.* **2008**, *47*, 9814–9859.

(14) Zi, J. C.; Valiente, J.; Zeng, J.; Zhan, J. X. *J.* Metabolism of quercetin by *Cunninghamella elegans* ATCC 9245. *Biosci. Bioeng.* **2011**, *112*, 360–362.

(15) Tronina, T.; Bartman´ska, A.; Milczarek, M.; Wietrzyk, J.; Popłon´ski, J.; Rój, E.; Huszcza, E. Antioxidant and antiproliferative activity of glycosides obtained by biotransformation of xanthohumol. *Bioorg. Med. Chem. Lett*. **2013**, *23*, 1957–1960.

(16) Wang, C.; Huo, X. K.; Zhang, B. J.; Sun, C. P.; Tian, X. G.; Deng, S.; Li, B.; Wang, W.; Dong, P. P.; Ma, X. C. Highly regioselective glucosylation of alcoholic hydroxyls of protostane triterpenoids mediated by fungal biotransformation. *Catal. Commun*. **2017**, *89*, 40–43.

(17) Kim, H. J.; Park, H. S.; Lee, I. S. Microbial transformation of silybin by *Trichoderma koningii*. *Bioorg. Med. Chem. Lett*. **2006**, *16*, 790–793.

(18) Vendrell, M.; Zhai, D. T.; Er, J. C.; Chang, Y. T. Combinatorial strategies in fluorescent probe development. *Chem. Rev.* **2012**, *112*, 4391–4420.

(19) Ueno, T.; Nagano, T. Fluorescent probes for sensing and imaging. *Nat. Methods* **2011**, *8*, 642–645.

(20) Lou, Z. R.; Li, P.; Han, K. L. Redox-responsive fluorescent probes with different design strategies. *Acc. Chem. Res.* **2015**, *48*, 1358–1368.

(21) Lee, M. H.; Kim, J. S.; Sessler, J. L. Small molecule-based ratiometric fluorescence probes for cations, anions, and biomolecules. *Chem. Soc. Rev*. **2015**, *44*, 4185–4191.

(22) Liu, H. W.; Liu, Y. C.; Wang, P.; Zhang, X. B. *Methods Appl. Fluores*. **2017**, *5*, 012003.

(23) Mao, G. J.; Wei, T. T.; Wang, X. X.; Huan, S. Y.; Lu, D. Q.; Zhang, J.; Zhang, X. B.; Tan, W. H.; Shen, G. L.; Yu, R. Q. High-sensitivity naphthalene-based two-photon fluorescent probe suitable for direct Bioimaging of H_2S in living cells. *Anal. Chem*. **2013**, *85*, 7875–7881.

(24) Liu, H.W.; Li, K.; Hu, X. X.; Zhu, L.; Rong, Q.; Liu, Y.; Zhang, X. B.; Hasserodt, J.; Qu, F. L.; Tan, W. In situ localization of enzyme activity in live cells by a molecular probe releasing a precipitating fluorochrome. *Angew. Chem. Int. Ed.* **2017**, *56*, 11788–11792.

(25) Zhao, Y.; Zhang, X. B.; Han, Z. X.; Qiao, L.; Li, C. Y.; Jian, L.; Shen, G. L.; Yu, R. Q. A highly sensitive and selective colorimetric and OFF-ON fluorescent chemosensor for Cu^{2+} in aqueous solution and living cells. *Anal. Chem.* **2009**, *81*, 7022–7030.

(26) Han, Z. X.; Zhang, X. B.; Qiao, L.; Li, C. Y.; Jian, L.; Shen, G. L.; Yu, R .Q. Efficient fluorescence resonance energy transfer-based ratiometric fluorescent cellular imaging probe for Zn^{2+} using a rhodamine spirolactam as a trigger. *Anal. Chem.* **2010**, *82*, 3108–3113.

(27) Zhu, B.; Gao, C.; Zhao, Y.; Liu, C.; Li, Y.; Wei, Q.; Ma, Z.; Du, B.; Zhang, X. A 4-hydroxynaphthalimide-derived ratiometric fluorescent chemodosimeter for imaging palladium in living cells. *Chem. Commun.* **2011**, *47*, 8656–8658.

(28) Silvers, W. C.; Prasai, B.; Burk, D. H.; Brown, M. L.; McCarley, R. L. Pro-fluorogenic reductase substrate for rapid, selective, and sensitive visualization and detection of guman cancer cells that overexpress NQO1. *J. Am. Chem. Soc.* **2013**, *135*, 309–314.

(29) Hou, X. F.; Yu, Q. X.; Zeng, F.; Yu, C. M.; Wu, S. Z. Ratiometric fluorescence assay for *γ*-glutamyltranspeptidase detection based on a single fluorophore via analyte-induced variation of substitution. *Chem. Commun.* **2014**, *50*, 3417–3420.

(30) Zhu, B.; Li, P.; Shu, W.; Wang, X.; Liu, C.; Wang, Y.; Wang, Z.; Wang, Y.; Tang, B. Highly specific and ultrasensitive two-photon fluorescence imaging of native HOCl in lysosomes and tissues based on thiocarbamate derivatives. *Anal. Chem.* **2016**, *88*, 12532–12538.

(31) Zhang, X. X.; Wu, H.; Li, P.; Qu, Z. J.; Tan, M. Q.; Han, K. L. A versatile two-photon fluorescent probe for ratiometric imaging *E. coli β*-galactosidase in live cells and in vivo. *Chem. Commun.* **2016**, *52*, 8283–8286.

(32) Lv, X.; Ge, G. B.; Feng, L.; Troberg, J.; Hu, L. H.; Hou, J.; Cheng, H. L.; Wang, P.; Liu, Z. M.; Fine, M.; Cui, J. N.; Yang. L. An optimized ratiometric fluorescent probe for sensing human UDPglucuronosyltransferase 1A1 and its biological applications. Biosens. Bioelectron. 2015, 72, 261–267.

(33) Lv, X.; Feng, L.; Ai, C. Z.; Hou, J.; Wang, P.; Zou,L. W.; Cheng, J.; Ge, G. B.; Cui, J. N.; Yang, L. A practical and high-affinity fluorescent probe for uridine diphosphate glucuronosyltransferase 1A1: a good surrogate for bilirubin. *J. Med. Chem.* **2017**, 60, 9664−9675.

(34) Wu, X. F.; Li, L. H.; Shi, W.; Gong, Q. Y.; Li, X. H.; Ma, H. M. Sensitive and selective ratiometric fluorescence probes for detection of intracellular endogenous monoamine oxidase A. *Anal. Chem*., **2016**, *88*, 1440–1446.

(35) Tian, X.; Huo, X.; Dong, P.; Wu, B.; Wang, X.; Wang, C.; Liu, K.; Ma, X. Sulfation of melatonin: enzymatic characterization, differences of organs, species and genders, and bioactivity variation. *Biochem. Pharmacol*. **2015**, *94*, 282−296.

(36) Sun, Q.; Harper, T. W.; Dierks, E. A.; Zhang, L.; Chang, S.; Rodrigues, A. D.; Marathe, P. 1-aminobenzotriazole, a known cytochrome P450 inhibitor, is a substrate and inhibitor of N-acetyltransferase. *Drug Metab. Dispos.* **2011**, *39*, 1674–1679.

(37) Zhang, R.; Cui, Y.; Wang, Y.; Tian, X.; Zheng, L.; Cong, H.; Wu, B.; Huo, X.; Wang, C.; Zhang, B.; Wang, X.; Yu, Z. Catechol-O-methyltransferase and UDP-glucuronosyltransferases in the

metabolism of baicalein in different species. *Eur. J. Drug. Metab. Pharmacokinet.* **2017**, *6*, 981−992.
(38) Mai, Z. P.; Zhou, K.; Ge, G. B.; Wang, C.; Huo, X. K.; Dong, P. P.; Deng, S.; Zhang, B. J.; Zhang, H. L.; Huang, S. S.; Ma, X. C. Protostane triterpenoids from the rhizome of *Alisma orientale* exhibit inhibitory effects on human carboxylesterase 2. *J. Nat. Prod.* **2015**, *78*, 2372−2380.
(39) Hettiarachchi, S. U.; Prasai, B.; McCarley, R. L. Detection and cellular imaging of human cancer enzyme using a Turn-On, wavelength-shiftable, self-immolative Pro-fluorophore. *J. Am. Chem. Soc.* **2014**, *136*, 7575–7578.
(40) Xie, K. B.; Dou, X. X.; Chen, R. D.; Chen, D. W.; Fang, C.; Xiao, Z. Y.; Dai, J. G. Two novel fungal phenolic UDP glycosyltransferases from *Absidia coerulea* and *Rhizopus japonicas*. *Appl. Environ. Microbiol.* **2017**, *83*, 3103–3116.
(41) Ye, M.; Dai, J. G.; Guo, H. Z.; Cui, Y. J.; Guo, D. A. Glucosylation of cinobufagin by cultured suspension cells of *Catharanthus roseus*. *Tetrahedron Lett*. **2002**, *43*, 8535–8538.
(42) Yang, L.; Wang, Z. H.; Lei, H.; Chen, R. D.; Wang, X. L.; Peng, Y.; Dai, J. G. Neuroprotective glucosides of magnolol and honokiol from microbial-specific glycosylation. *Tetrahedron* **2014**, *70*, 8244–8251.
(43) Yehia, R. S.; Ali, E. M.; Al-Zahrani, A. Feasibility of oleaginous fungi isolated from soil samples of Saudi Arabia for mycodiesel production. *Appl. Biochem. Biotechnol.* **2017**, *53*, 94–100.

for TOC only

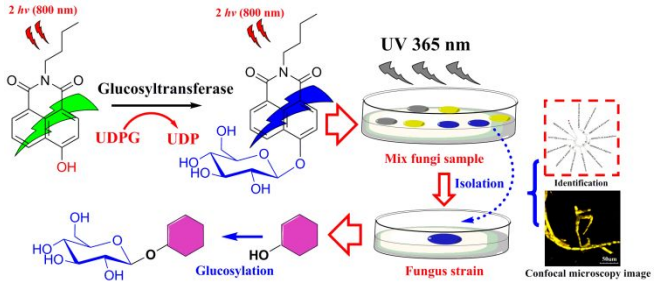
2 hv (800 nm)
Glucosyltransferase
UDPG
UDP
2 hv (800 nm)
UV 365 nm
Mix fungi sample
Isolation
Identification
Confocal microscopy image
Fungus strain
Glucosylation